Vaccine xxx (xxxx) xxx

Contents lists available at ScienceDirect

Vaccine

journal homepage: www.elsevier.com/locate/vaccine

Antigenic and physicochemical characterization of Hepatitis B surface protein under extreme temperature and pH conditions

J.L.S. Lopes [a,*], D.C.A. Oliveira [b], C.L.A. Utescher [b], W. Quintilio [b], E.C.N. Tenório [b], C.L.P. Oliveira [a], M.C.A. Fantini [a], M.K. Rasmussen [c,d], H.N. Bordallo [c,e], O.A. Sant'Anna [b], V.F. Botosso [b]

[a] Institute of Physics, University of São Paulo, São Paulo, Brazil
[b] Butantan Institute, São Paulo, Brazil
[c] Niels Bohr Institute, University of Copenhagen, Copenhagen, Denmark
[d] Department of Health Technology, Technical University of Denmark, Lyngby, Denmark
[e] European Spallation Source, Lund, Sweden

ARTICLE INFO

Article history:
Received 7 May 2019
Received in revised form 22 August 2019
Accepted 2 September 2019
Available online xxxx

Keywords:
Hepatitis B
HBsAg antigenicity
Thermal stability
pH stability

ABSTRACT

Hepatitis B virus causes acute and chronic infections in millions of people worldwide and, since 1982, a vaccine with 95% effectiveness has been available for immunization. The main component of the recombinant hepatitis B vaccine is the surface antigen protein (HBsAg). In this work, the effect of pH, ionic strength and temperature on the native state of the HBsAg antigen were studied by a combination of biophysical methods that included small angle X-ray scattering, synchrotron radiation circular dichroism, fluorescence and surface plasmon resonance spectroscopies, as well as in vivo and in vitro potency assays. The native conformation, morphology, radius of gyration, and antigenic properties of the HBsAg antigen demonstrate high stability to pH treatment, especially in the pH range employed in all stages of HBsAg vaccine production and storage. The HBsAg protein presents thermal melting point close to 56 °C, reaching a more unfolded state after crossing this point, but it only experiences loss of vaccine potency and antigenic properties at 100 °C. Interestingly, a 6-month storage period does not affect vaccine stability, and the results are similar when the protein is kept under refrigerated conditions or at room temperature (20 °C). At frozen temperatures, large aggregates (>200 nm) are formed and possibly cause loss of HBsAg content, but that does not affect the in vivo assay. Furthermore, HBsAg has a well-ordered secondary structure content that is not affected when the protein is formulated with silica SBA-15, targeting the oral delivery of the vaccine. The combined results from all the characterization techniques employed in this study showed the high stability of the antigen at different storage temperature and extreme values of pH. These findings are important for considering the delivery of HBsAg to the immune system via an oral vaccine.

1. Introduction

Hepatitis B is a serious acute and chronic viral disease, which affects millions of people, causing occupational hazards, cirrhosis, hepatocellular carcinoma and death, as pointed out by the World Health Organization (WHO). The Global Health Sector Strategy (GSS) established the plan for the elimination of viral hepatitis as a major public health threat by 2030, reducing new infections by 90% and mortality by 65% [1]. To achieve this goal, the WHO recommends universal immunization of infants, adolescents and adults, and considers the vaccination of infants and the prevention of mother-to-child transmission as a priority [2]. Since 1982, a 95%-effective vaccine has been available, firstly based on the smaller non-infectious sub-viral particles (SVPs) purified from the plasma of chronically infected patients, which were completely replaced by recombinant vaccines over the years [3,4]. The main component of the recombinant hepatitis B vaccine is the surface antigen (HBsAg), a protein that self-assembles into ~22 nm spherical virus-like particles (VLPs) which contain lipids, derivative from the host cell, and around 80–100 monomers of HBsAg in a particle [5]. The VLP based vaccine is safe and effective, but it is clear that maintaining the native conformation of the main epitopes within the VLP antigen in all stages of production and storage is critical for its effectiveness. One of the biggest problems of hepatitis B VLPs is the phenomenon of aggregation that may occur during the

* Corresponding author at: Rua do Matão 1371, 05508-090 São Paulo, Brazil.
E-mail address: zeluiz@if.usp.br (J.L.S. Lopes).

https://doi.org/10.1016/j.vaccine.2019.09.005
0264-410X/

production process as well as during storage and it can be associated with loss of vaccine potency [6,7]. Although the Hepatitis B vaccine has been described as relatively stable to temperature variations around room temperature [8], for instance even after 1 month at 37 °C, the exposure to elevated temperatures should be avoided [9–11]. On the other hand, the freezing effects on the HBsAg protein are not yet totally understood, although dissociation of the antigen from the adjuvant surface and structural damage to the antigen have been detected on vaccines that use aluminum salt adjuvants. Therefore, the recommendation for the storage and transport of the recombinant vaccine is between 2 and 8 °C [10,12–14].

Currently, the immunization schedule comprises 3 intramuscular doses, however, the implementation of alternative delivery routes of Hepatitis B vaccine has the potential to greatly improve the extent and efficiency of global vaccination programs. Oral administration is an interesting approach because it improves delivery and transportation, potentially reducing costs and improving vaccine coverage. Since the early researches on the Hepatitis B oral vaccine [15,16], many recent results have been reported with different organic and inorganic vehicles/adjuvants, essential to produce humoral response [17–22]. Among these materials, ordered mesoporous silica (OMS) scaffolds have been successfully used to encapsulate antigens [23–25], including Hepatitis B surface Antigen (HBsAg) [21] for oral vaccine delivery. New nanomaterials, like the hexagonal mesoporous silica structures (SBA-15) [26], have also been extensively investigated aiming at a variety of biomedical applications [27–30]. Recently, the localization and dynamics of the HBsAg inside the SBA-15 and its efficacy as a vehicle for oral vaccination have been demonstrated [31]. Thus, to better understand how SBA-15 works as a protective vehicle through the acid environment of the stomach and duodenum regions it is important to know the effects of pH variation on the protein. This variation could compromise the disulfide bonding of the antigen altering its immunogenicity [32].

In addition, during the manufacturing process, the HBsAg is submitted to different pH and ionic strength conditions. In this study, we performed a physicochemical and antigenic characterization of HBsAg in different conditions to simulate the manufacturing steps and diverse storage temperatures. To this end, small angle X-ray scattering (SAXS), synchrotron radiation circular dichroism (SRCD) and fluorescence spectroscopies were employed to investigate the structural characteristics and properties of HBsAg under various conditions. SAXS is a very useful technique to determine the overall size and shape of proteins [33] for investigations directly in solution, while SRCD is a powerful tool to determine protein secondary structure integrity under real conditions [34]. SRCD can also be used to scrutinize secondary structures and to perform fold recognition and structural genomics [34]. Here, SRCD was crucial to determine the influence of pH and temperature on the biophysical properties of the HBsAg antigen. Finally, fluorescence spectroscopy was employed to investigate the microenvironment of the Tryptophan (Trp) residues in HBsAg in different media, and in vivo and in vitro potency assays were done to access the stability of HBsAg in different conditions.

2. Materials and methods

2.1. Recombinant HBsAg

Produced in yeast, the high purified Hepatitis B surface antigen (HBsAg) is the active principle of hepatitis B vaccine produced by Butantan Institute [35]. This antigen in bulk is kept in PBS [phosphate-buffered saline under pH = 7.0] (pH 7.0 – ranging from 7.0 to 7.4) at 4 °C until formulation with addition of preservative (thimerosal 0.10 mg/ml) and absorbed to aluminum hydroxide adjuvant (1.25 mg/ml). In the present study we used only the antigen in bulk preserved in the same conditions before the final formulation.

2.2. Sample preparation

Samples of 10 mL of the bulk were prepared using Amicon Ultra-15 Centrifugal Filter Units (50 kDa) in a final protein concentration of 450 μg/mL. The original PBS was changed to different solutions that are routinely used during the production process of Hepatitis B vaccine. The solutions used were: i) solutions used in intermediate products: sodium phosphate 10 mM, pH 5.5, 6.0, 6.4, 7.0 and 8.5; ii) buffer used in the formulation of pentavalent vaccine [(Diphtheria, Tetanus, Pertussis, Hepatitis B and Haemophilus influenza vaccine): sodium/potassium buffer with 150 mM NaCl pH 6.4, called in this work pH 6.4 T. In addition, HBsAg was formulated with silica SBA-15 in proportion of 10:1 (5000 μg of silica and 500 μg of HBsAg) [21]. Samples were stored for 6 months at 3 different conditions: −20 °C, 4 °C and for 5 consecutive days at room temperature (~20 °C) followed by storage at 4 °C. They were tested shortly after preparation (T0) and after 6 months (T6). As recommended by WHO, for the in vivo and in vitro assays used as a control of protein denaturation, the original bulk (PBS, pH 7.0) was heated at 60 °C for 7 days to artificially reduce the potency of vaccine [12]. In addition, in this study we heated the sample at 100 °C for the same period. SBA-15 was synthesized as described in Ref. [26].

2.3. Analytical methods for HBsAg determination

2.3.1. Assay for in vitro antigenicity of HBsAg by ELISA

The concentration of HBsAg was determined using a quantitative sandwich ELISA (Murex HBsAg Version 3, DiaSorin) following the manufacturer's instruction. In short, the specimen is pre-incubated in microwells coated with a mixture of mouse monoclonal antibodies specific for diverse epitopes on the 'a' that is described as a specific conformation of the antigenic loop polypeptide of HBsAg. Affinity purified goat antibody to HBsAg conjugated to horseradish peroxidase is then added to the specimen in the wells. 3,3′,5,5′-tetramethylbenzidine (TMB) and hydrogen peroxide were used as a substrate for color development and optical density was ready at 450 nm. Triplicate vial were used by each condition. Estimations of the antigenic content were determined using CombiStats™ software (version 4.0; EDQM/Council of Europe) by Finney's Parallel line assay. Antigenicity of each condition was expressed as a percentage (%) of the HBsAg amount measure in the reference control (HBsAg in PBS, pH 7.0).

2.3.2. Other analytical methods

Total protein concentrations were determined by Lowry methodology [36]. SDS-PAGE analysis of protein was done as described by Laemmli et al. [37] using 12% polyacrylamide gel. The test was performed with 1–2 μg of each sample in denaturant conditions and stained by $AgNO_3$.

2.4. Assay for in vitro antigen-antibody interaction by surface plasmon resonance (SPR) instrumentation

Steady state affinity was determined by surface plasmon resonance in Biacore T200 System (GE Life Sciences). Anti-mouse IgG (Mouse Antibody Capture Kit, BR-1008-38, GE Life Sciences) was immobilized onto a CM5 sensorchip by amino coupling accordingly to supplier instructions. Hepatitis B Virus surface monoclonal antibodies: HB3 (cat. number MA1-19263); HB5 (cat. number MA1-19264) and I64I (cat. number MA1-7350) were purchased

Please cite this article as: J. L. S. Lopes, D. C. A. Oliveira, C. L. A. Utescher et al., Antigenic and physicochemical characterization of Hepatitis B surface protein under extreme temperature and pH conditions, Vaccine, https://doi.org/10.1016/j.vaccine.2019.09.005

from Invitrogen/ThermoFisher. Monoclonal antibodies at 10 μg/mL in HBS-EP running buffer (0.01 M Hepes pH 7.4, 0.15 M NaCl – with 3 mM EDTA and 0.005% Tween 20 – HBS-EP, GE Life Sciences) was then captured on the sensor (10 μL/min, 90 s) and this activated surface was used to assess steady state affinity of each mAb to the different samples of HBsAg. Protein concentrations from 2.5 to 40 μg/mL (twofold dilutions) were applied in a single cycle approach (30 μL/min, contact 120 s), followed by a regeneration pulse of 15 μL of 10 mM Glycine (pH 1.7). The affinities were calculated by BiaEvaluation software version 3.0.

2.5. In vivo potency assay

Animal tests were performed in accordance with institutional guidelines for animal welfare under Instituto Butantan Animal Care and Use Committee permits no. 1527091117. Female BALB/c mice (*Mus musculus*) aged 5 weeks and weighting from 17 to 22 g were provided by Instituto Butantan Animal Facilities. All the animals were from the same stock, and during the experiments, they received balanced food and fresh water ad libitum. Groups of 5 mice were immunized intraperitoneally (0.5 mL) with a final concentration of 1.25 μg/mL of HBsAg diluted in PBS [phosphate-buffered saline pH 7.0] adsorbed in 0.5 mg/ml of aluminum hydroxide. All the HBsAg samples were prepared the same way for immunization. Terminal bleeds were taken after 30 days from retro-venous orbital plexus. Individual sera were tested for antibodies to HBsAg by ELISA assay as described in Scaramuzzi et al. [21]. Titers are given as the reciprocal of the calculated sample dilution corresponding to optical density (OD) above the calculated cut off (mean of OD) of three negative control sera plus 2 standard deviations (SD)). Wilcoxon Statistical test was used to analyze the results. One group was immunized with PBS as a negative control. Non-responder is defined as a mouse having a titer below 1 on a 10 log base. The concentration of HBsAg was determined using a quantitative sandwich ELISA (Murex HBsAg Version 3, DiaSorin) following the manufacturer's instructions. Triplicate vial were used in each condition. Estimations of the antigenic content were determined using CombiStats™ software (version 4.0; EDQM/Council of Europe) by Finney's Parallel line assay.

2.6. Small angle X-ray scattering (SAXS)

SAXS measurements on HBsAg were performed on a laboratory instrument XEUSS (Xenocs) SAXS instrument with a wavelength of 1.54 Å and sample to detector distance of 0.9 m. At this configuration the measured q range covers 0.015 $Å^{-1}$ and 0.43 $Å^{-1}$. The measurements were performed on samples stored at different temperatures and also subjected to three different adjusted pH values (5.5, 7.0 and 8.5). All measurements were performed at room temperature (25 °C). PBS and water were measured as a background and a standard for obtaining the absolute scattering intensity [38]. The sample concentrations were 0.45 mg/mL. The data was analyzed using the inverse Fourier Transform (IFT) method [39] to obtain the forward scattering (I(0)), pair distance distribution and radius of gyration of HBsAg using the software package WIFT [38] and GNOM [40]. For the *ab initio* modeling, the DAMMIN program [41] was used. This program works as follows: a search space filled with dummy atoms is created with a diameter identical to the one obtained from IFT analysis. Therefore, the particle should be enclosed in this volume. By using a Monte Carlo based heuristic optimization (simulated annealing) a subset of this initial search space is obtained. The obtained model provides the best fit of the experimental data.

2.7. Dynamic light scattering (DLS)

DLS measurements of HBsAg were performed at a 90Plus™ tabletop equipment from Brookhaven at three different adjusted pH values (5.5, 7.0 and 8.5) and storage temperatures (−20 °C, 4 °C and 20 °C). The correlation functions were modeled using the Non-Negative Least Squares (NNLS) method [42] available with the equipment software. As a result, the size distributions as a function of particle diameter are obtained. The size distributions can be weighted by the number of particles, particle volume or the volume squared (intensity). It is very useful to plot these three distributions in the same graph since it allows the identification of small fractions of large particles or contaminants.

2.8. Synchrotron radiation circular dichroism (SRCD) spectroscopy

The SRCD spectra of HBsAg (25 μM) in PBS (pH 7.0) or incorporated into the ordered mesoporous silica SBA-15 at PBS (pH 7.0) were collected over the wavelength range between 170 and 280 nm, in 1 nm intervals, using a 0.0106 cm pathlength quartz cuvette (Hellma Scientific), collecting 3 individual scans of each sample, at 10 °C, on the AU-CD beamline at the ASTRID2 synchrotron (University of Aarhus, Denmark). The structural stability of HBsAg was investigated over the temperature range between 10 and 90 °C, in 5 °C increment, allowing 5 min equilibration at each temperature, and alternatively, with the samples after storage at 25 °C and 4 °C for 5 successive days. In addition, samples prepared at different pHs (5.5, 6.0, 6.4, 7.0 and 8.5) and stored at 4 °C were analyzed when prepared (T0) and after 6 months (T6). Additionally, in order to investigate the protein structure after dehydration and examine the secondary structure of HBsAg after the removal of bulk water during formation of a protein film, the SRCD spectrum of a partially dehydrated film of HBsAg (0.7 nmol) deposited on the surface of a quartz glass plate was collected in the wavelength range between 155 nm and 280 nm, at 10 °C, with successive rotations on the plate (at 0°, 90°, 180° and 270°). The high tension (HT) signal (or dynode voltage) was collected simultaneously with each SRCD spectrum over the same wavelength range.

CDToolX software [43] was used for all SRCD data processing, which consisted of averaging the three individual scans, subtraction of the corresponding baseline spectrum, smoothing with a Savitzky-Golay filter, zeroing spectra in the 263–270 nm region and conversion to delta epsilon (Δε) units, using a mean residual weight of 112.8. Analysis of the HBsAg structural content was performed with the DICHROWEB server [44], using database SP175 [45] and the Continll [46] algorithm. Predictions of secondary structure of HBsAg were performed with GOR4 software [47]. Protein concentration was determined using the theoretical extinction coefficient of 81,315 M^{-1} cm^{-1} at 280 nm.

2.9. Intrinsic tryptophan (Trp) fluorescence spectroscopy

The steady-state emission spectrum of HBsAg (3.0 μM, a low concentration solution for obtaining the emission spectra, avoiding inner filter effects) in PBS (pH 7.0) or incorporated into SBA-15 particles, and alternatively, at the pH range between 5.5 and 8.5, were measured on an ISS K2 spectrofluorimeter (ISS Inc., Champaign, IL) using 8 nm slits for both excitation and emission and 1 cm pathlength quartz cuvettes. Sample excitation was performed at 295 nm and emission spectra were recorded from 300 to 450 nm, in 1 nm intervals, at a temperature ranging from 10 °C to 45 °C, using the temperature control via a circulating water bath.

Please cite this article as: J. L. S. Lopes, D. C. A. Oliveira, C. L. A. Utescher et al., Antigenic and physicochemical characterization of Hepatitis B surface protein under extreme temperature and pH conditions, Vaccine, https://doi.org/10.1016/j.vaccine.2019.09.005

3. Results and discussion

The production process of the Hepatitis B vaccine by the Butantan Institute is comprised of several steps including fermentation, extraction and purification aiming to obtain a highly purified HBsAg VLPs in PBS at neutral pH. During all these steps, the antigen is submitted to different conditions of pH, varying from 5.5 to 8.5 and ionic strength, with or without NaCl. The effects of the components of these different solutions were analyzed regarding the structural protein integrity (both secondary and tertiary), antigenicity and immunogenicity.

3.1. SAXS characterizations of HBsAg in aqueous solution

As shown in previous works the HBsAg protein forms a stable self-assemble on VLPs with a small degree of polydispersity. Several modeling approaches were tried to describe the scattering data, either assuming a shape or model-free methods. The best results were obtained using the so-called IFT method (Indirect Fourier transformation method), were a pair distribution function (p(r)) is obtained from the fitting of the experimental data. However, since the system can have a certain degree of polydispersity, is necessary to understand what the obtained p(r) may provide. For a system composed of different non-interacting particles, the total scattering intensity is given by [48]:

$$I(q)_{tot} = \sum_{i=1}^{N} c_i I_i(q) \quad (1)$$

were c_i stands for the concentration of the particles i in the system. The pair distribution function p(r) can be obtained by the Fourier transform of the scattering intensity I(q) from a system composed of non-interacting identical particles [49]:

$$p(r) = \frac{1}{2\pi^2} \int_0^{\infty} rqI(q)sen(qr)dq \quad (2)$$

Since each fraction of Eq. (1) is assumed to be monodisperse, one can apply a Fourier transform in both sides of that equation an define a total p(r) as

$$p(r)_{tot} = \sum_{i=1}^{N} c_i p_i(r) \quad (3)$$

Therefore, the total p(r) function, which can be directly calculated form the total scattering intensity, can be understood as the composition of the individual p(r) functions of each fraction. In this way, this provides an average representation of the particles composing the system. For small degrees of polydispersity (in size and shape) this average p(r) function gives a good indication of the overall size and shape of the particles in the system. This approach was successfully used in previous investigations [31].

Absolute scattering intensity data, fitted using the IFT method, are shown in Figs. 1 and 2 for samples measured with various storage temperatures (−20 °C, 4 °C and 25 °C) and pH (5.5, 7.0 and 8.5). The pair distance distribution p(r) for each case is shown in Figs. 1b and 2b. The obtained p(r) functions indicate an overall globular shape for all the investigated cases. The Guinier plots (Ln I × q^2) are shown in Suppl. Fig. 1. As shown in that plot, one has a reasonable linear region on at low angles which indicates a certain degree of monodispersity in the samples. The obtained radius of gyration from the Guinier analysis are similar to the ones obtained from the IFT procedure. It is necessary to note that the experimental q range is not optimum for the investigated particle sizes (~30 nm), which would demand a $q_{min} < 0.104\ nm^{-1}$ (π/30). In any case, since the p(r) is obtained from the fitting of the full experimental curve, it is possible to obtain good extrapolations even in these situations [50]. The sizes obtained by the SAXS analysis are much larger than the expected for the protein monomer. This was also confirmed by the estimation of the average molecular weight (MW) of 1700–2800 kDa of the studied samples, obtained by the forward scattering [38]. As the theoretical MW of the HBsAg protein is 25387.14 Da, one can estimate that the VLPs are composed of oligomers ranging from 70 to 110 protein subunits in a given particle. The obtained parameters from IFT fit are shown in Table 1.

Another strategy can be used to obtain a possible indication of the overall shape of the formed VLP. Even though the atomic resolution structure for the investigated protein is not available, it is possible to calculate the minimum radius of a protein in order to have a given molecular weight. As shown by Erickson [51], the

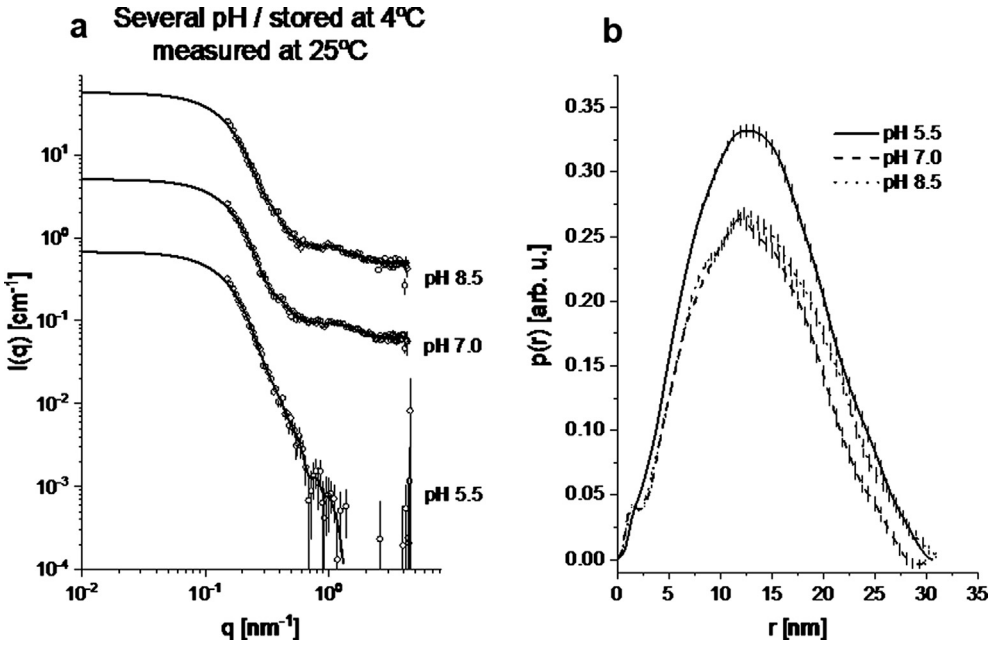

Fig. 1. SAXS results for HBsAg samples initially stored at 4 °C prepared at pH 5.5, 7.0, and 8.5. (a) SAXS intensities (symbols) and IFT fits (solid lines). The curves where shifted for an easier visualization. (b) Pair distance distribution – p(r) functions obtained from IFT fits.

Please cite this article as: J. L. S. Lopes, D. C. A. Oliveira, C. L. A. Utescher et al., Antigenic and physicochemical characterization of Hepatitis B surface protein under extreme temperature and pH conditions, Vaccine, https://doi.org/10.1016/j.vaccine.2019.09.005

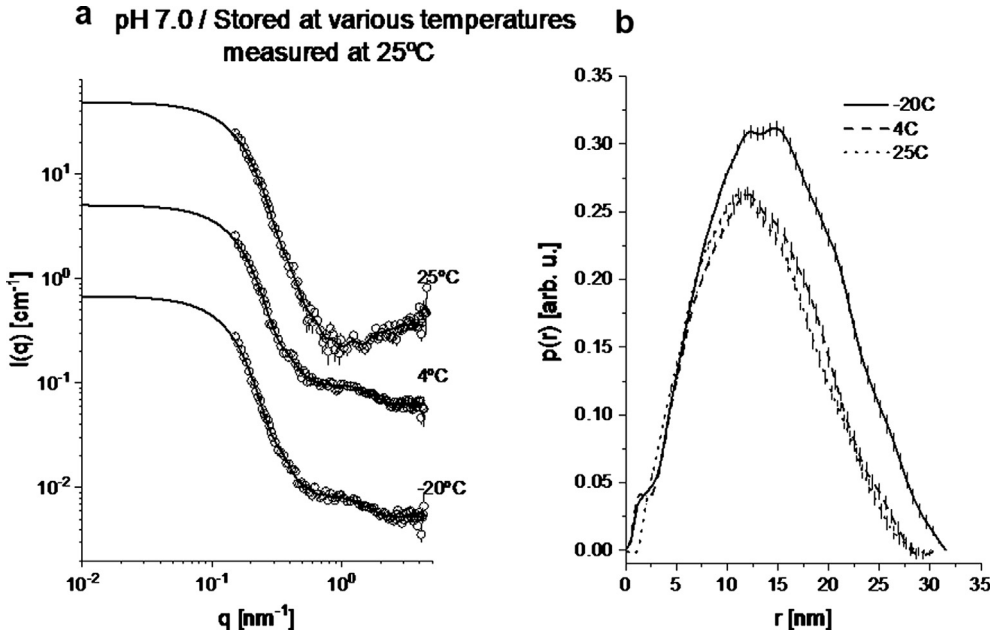

Fig. 2. SAXS results for HBsAg samples prepared at pH 7.0 and stored initially stored at −20 °C, 4 °C and 25 °C. (a) SAXS intensities (symbols) and IFT fits (solid lines). The curves where shifted for an easier visualization. (b) Pair distance distribution – p(r) – functions obtained from IFT fits.

Table 1
Structural parameters obtained from IFT fitting.

	pH 7.0			pH 5.5	pH 8.5
	Storage			Storage	
Parameter	−20 °C	4 °C	25 °C	4 °C	4 °C
R_g [nm]	11.3 ± 0.1	10.1 ± 0.2	10.7 ± 0.1	11.2 ± 0.1	10.9 ± 2
D_{max} [nm]	~31.5	~30.5	~30.8	~32.5	~31.5
MW [MDa]	2.3 ± 0.2	1.7 ± 0.2	2.3 ± 0.2	2.8 ± 0.3	1.9 ± 0.2
N prot	~90	~70	~90	~110	~70

minimum radius of a protein can be calculated by the relationship Rmin = 0.066 $MW^{1/3}$, for MW in Da and Rmin in nanometer. Therefore, for the HBsAg protein, MW = 25387.14 Da, which gives Rmin ~ 1.93 nm. This is, of course, a very crude approximation for the protein, but this presumed sphere has a volume similar to the protein. This information was used in the *ab initio* calculations, where the subunit radius was assumed to be 2 nm. In this way, the obtained low-resolution model will give an indication of a possible oligomeric arrangement of the HBsAg protein monomers in the VLP. The obtained low resolution models for the samples at pH 7.0 are shown in Suppl. Fig. 2 together with the corresponding fit.

The radius of gyration (R_G) of HBsAg in all investigated samples is shown in Table 1. It is observed that R_G varies slightly on the investigated samples, i.e. between 10.1 nm and 11.3 nm.

3.2. Dynamic light scattering of HBsAg protein

The correlation functions, NNLS fit and obtained number, volume and intensity distributions are shown in Suppl. Figs. 3, 4, and 5, respectively. In all cases, the size distributions show a maximum around 30 nm, in very good agreement with the obtained values from the SAXS investigations. However, the distributions also indicate the presence of larger aggregates (>200 nm) in variable fractions, corroborating with the results obtained from SAXS (Suppl. Table 1). For the calculation of the given fractions, the area under the curve for the peaks at larger sizes and the area for the peak at lower sizes are normalized by the full area under the curve, which then gives the mass fraction, in percentage, of VLP (smaller sizes) and the larger aggregates in each case. It is important to note that these values are for volume fractions. If one computes the number of particles in each situation, they clearly see that the presence of VLP particles is above 99.8%. The obtained results indicate that the product stored at −20 °C tends to form a slightly larger amount of aggregates, which may be not recommended for maintenance of antigenic properties [13].

3.3. Secondary and tertiary structures of HBsAg protein in aqueous solution, incorporated into SBA-15 and in films

The SRCD spectrum of HBsAg in aqueous solution (Fig. 3) is typical of a protein containing regions in α-helix structure, which is assigned with the presence of the two minima at 208 nm and 220 nm, the large positive maximum at 192 nm, and an additional shoulder at 180 nm. Indeed, the deconvolution of HBsAg SRCD spectrum at pH 7.0 using DICHROWEB webserver gave a content of 24% helix, 21% β-strands and 55% other structures (turns and disordered). These values are in close agreement with the predictions of secondary structure (Suppl. Fig. 6a) performed on HBsAg (25% α-helix, 21% extended β-strand and 54% other structures) using bioinformatics analysis. In addition to that, the Trp emission spectrum of HBsAg, which contains 13 Trp and 6 Tyrosine (Tyr) residues in its primary structure, in aqueous solution at 10 °C (Fig. 3 inset), has maximum emission centered at 335 nm, typical

Please cite this article as: J. L. S. Lopes, D. C. A. Oliveira, C. L. A. Utescher et al., Antigenic and physicochemical characterization of Hepatitis B surface protein under extreme temperature and pH conditions, Vaccine, https://doi.org/10.1016/j.vaccine.2019.09.005

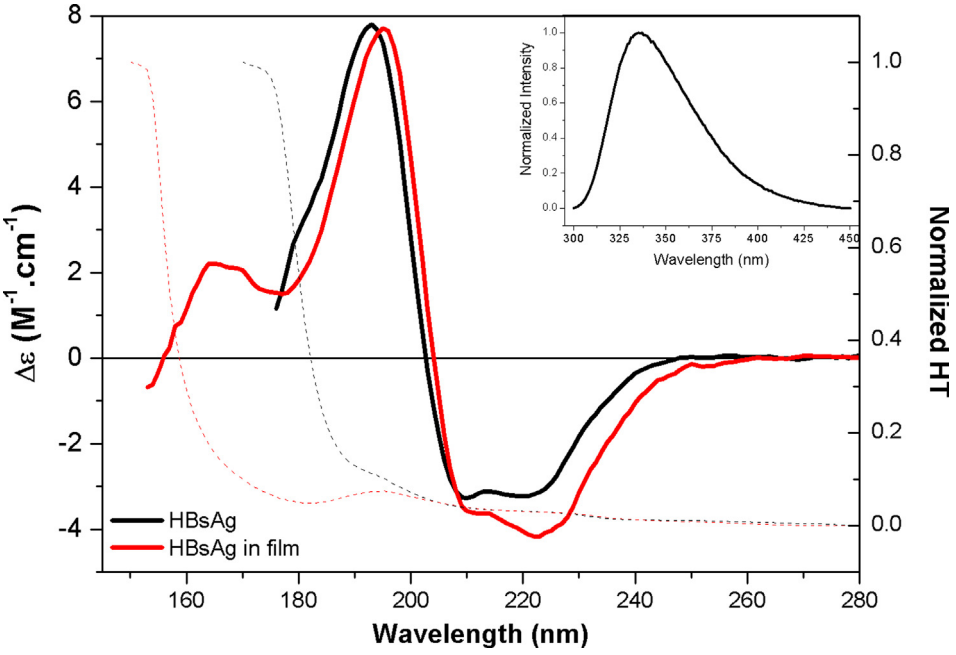

Fig. 3. (a) SRCD spectra of HBsAg in aqueous solution (pH 7.0, black curve) and deposited in a partially dehydrated film (red curve), and their respective HT curves (dashed line). Inset: Trp emission spectrum of HBsAg at 10 °C in aqueous solution (pH 7.0). (For interpretation of the references to color in this figure legend, the reader is referred to the web version of this article.)

of proteins in which the Trp residues are shielded from exposure to water molecules [52].

The SRCD spectrum of HBsAg incorporated into SBA-15 (Suppl. Fig. 6b) showed no detectable structural changes, suggesting that the native secondary structure of HBsAg was kept unaltered inside the silica matrix. Estimations of secondary structure content were equivalent to that of the protein in solution. In agreement with that, the Trp emission of the protected HBsAg presented the same maximum emission at 335 nm and showed the preservation of the aromatic residues' environment from solvent. As observed when the protein is adsorbed in aluminum salt for the formulation of the conventional Hepatitis B vaccine, the incorporation of HBsAg into silica did not affect the VLP, maintaining the integrity of important epitopes [53]. In addition, we emphasize that our group showed previously that HBsAg particles incorporated into SBA-15 induced the production of specific antibodies, by both oral and subcutaneous injection, demonstrating the maintenance of their immunogenicity properties and supporting our data [21].

Moreover, as often observed for well-ordered globular proteins during formation of a partially dehydrated film [34], the SRCD spectrum of the HBsAg in a partially dehydrated film is formed only by HBsAg and residual water (Fig. 3). Also, the result showed that the protein was able to maintain its native globular structure after removal of bulk water and revealed additional bands in the low-wavelength region (at 165 nm and 175 nm) that could be attributed to the presence of regions in β-strand conformation in the protein [34].

3.4. HBsAg stability at different pH and temperatures

After incubating HBsAg at pH ranging from 5.5 to 8.5, the respective SRCD (Fig. 4a) and Trp emission (Fig. 4b) spectra were taken and revealed no changes compared to HBsAg in PBS (pH 7.0), suggesting the high structural stability of HBsAg to preserve its native secondary structure and exposure of Trp region to water under this whole pH range. In fact, even after 6 months of storage (Suppl. Fig. 7) the SRCD spectra of HBsAg preserved the same spec-

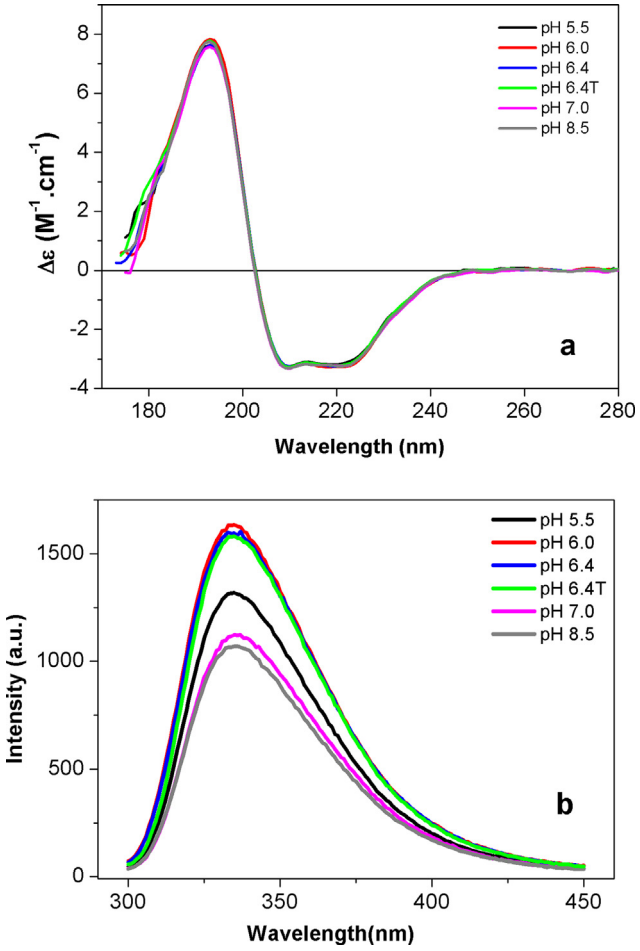

Fig. 4. (a) SRCD spectra of HBsAg at different pHs (from 5.5 to 8.5) and (b) their respective Trp emission spectra.

Please cite this article as: J. L. S. Lopes, D. C. A. Oliveira, C. L. A. Utescher et al., Antigenic and physicochemical characterization of Hepatitis B surface protein under extreme temperature and pH conditions, Vaccine, https://doi.org/10.1016/j.vaccine.2019.09.005

tral shape of the native protein. At the more acidic pHs, from 5.5 to 6.4, a slight reduction of the spectral bands was noted, however, without changing its spectral shape, suggesting that the native global structure of the antigen was preserved. The preserved structure of HBsAg was also suggested due to the same Trp emission maximum position after 6 months storage at the studied pH range.

To check the effect of temperature on the protein structure, a thermal melting assay was conducted on HBsAg in PBS (pH 7.0) until the complete denatured state was reached at 90 °C (Fig. 5a). Initially, the SRCD spectra of HBsAg kept at 4 °C taken at temperature values between 10 °C and 45 °C showed that the secondary structure of HBsAg presented no conformational changes from its native state. In agreement with that, fluorescence spectroscopy showed that the position of the Trp maximum emission was not changed within this temperature range (Fig. 5b), independently of pH (Suppl. Fig. 8). However, on further heating, a gradual reduction in the magnitudes of all the SRCD spectral bands is observed (Fig. 5c). These changes might induce the protein to a complete unfolded state after crossing a melting point at 56 °C. However, the thermal melting analyses conducted with samples kept at room temperature showed a 5 °C reduction on its thermal melting point (Fig. 5c) suggesting that the thermal stability of this sample was slightly reduced.

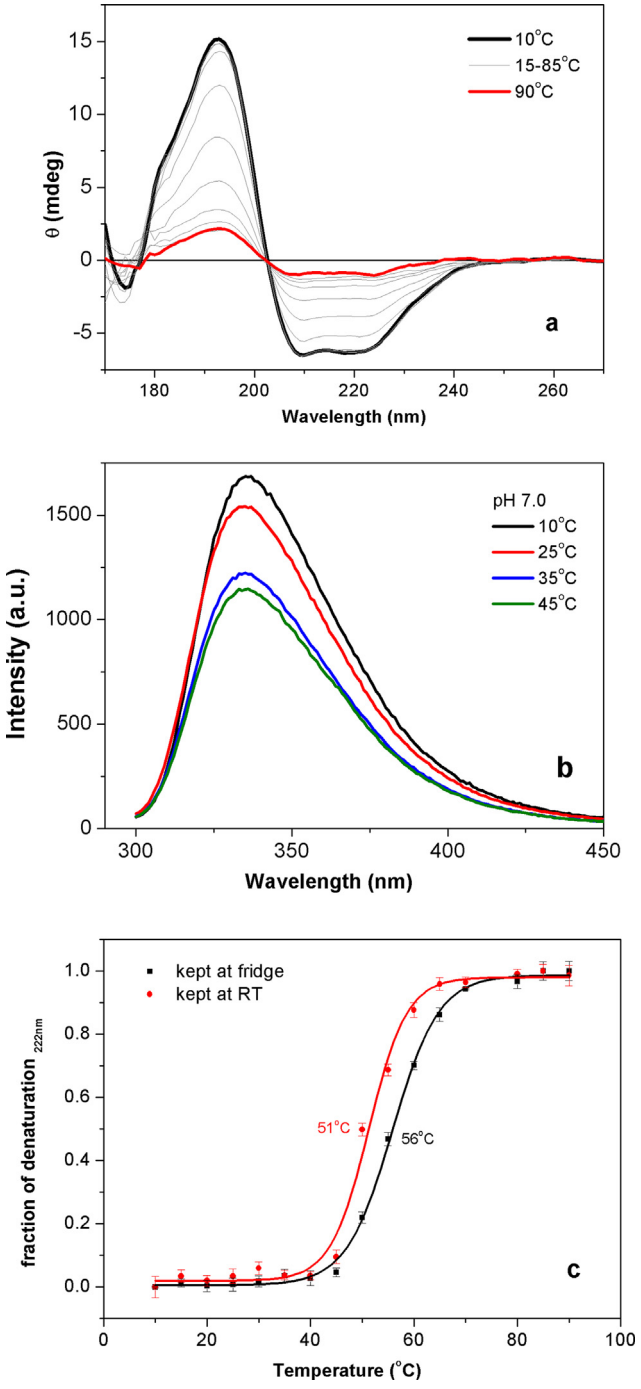

Fig. 5. (a) SRCD spectra collected upon thermal melting of HBsAg from 10 °C (black) to 90 °C (red), in 5 °C steps (intermediate scans are in gray). (b) Effect of temperature on the Trp emission spectrum of HBsAg between 10 and 55 °C. (c) Thermal denaturation curves of HBsAg taken from the ellipticity values at 222 nm from a sample kept either at 4 °C or at 25 °C.

Moreover, sequential SRCD spectra recorded from HBsAg kept at 4 °C followed by maintenance at room temperature (~20 °C) during five successive days (Suppl. Fig. 9) showed quite equivalent shape in all the spectral bands magnitude and position for the native conformation of HBsAg, even after 6 months storage. All these findings suggested no changes on the secondary structure of the protein within this time frame, showing high stability at 4 °C and at room temperature.

Taken together, the results revealed that the buffers employed during the manufacture and storage did not alter the native conformation of HBsAg, as revealed by the preservation of the SRCD spectral bands, the intrinsic Trp emission spectra and the value of radius of gyration, suggesting the quite high structural stability of this protein, even after 6 months storage. High temperature, however, was shown to have a more severe effect on protein denaturation, especially at values close to its melting point (56 °C). At more extreme pH values, a tendency to form large aggregates and/or protein unfolding was observed, and that could ultimately promote the loss of vaccine potency [6,53].

3.5. Antigenicity and immunogenicity results

The antigenicity of HBsAg was measured by ELISA using antibodies against the "a" determinant corresponding to residues 99–169 of the HBsAg protein, the immune-dominant region of the particle, eliciting the neutralization of antibody responses upon natural infection and vaccination. Hence maintenance of the structural conformation of the particle is crucial for the recognition by the antibodies [53–55]. Heating to extreme temperatures can cause serious morphology changes, coupled with inappropriate intra- and intermolecular disulfide bonds that are crucial for the immunochemical and biological function of the HBsAg particles and consequently for its antigenicity and immunogenicity properties [53]. Thus, as a control of denaturation, one sample of reference control (HBsAg in PBS – pH 7.0) was submitted to extreme temperature of 60 °C for 7 days. Although 60 °C is close to the melting temperature, and it is the temperature recommended by WHO [12], this temperature was not enough to complete denatured the HBsAg, corroborating the expected antigen stability in this temperature verified by others [53]. Consequently, the sample was submitted to a higher temperature (100 °C) through the same time leading to complete denaturation of the antigen, indicated by the loss of recognition by specific antibodies (Fig. 6 and Suppl. Fig. 10).

As showed in Fig. 7, the relative antigenicity of samples maintained at 4 °C in solutions with lower pH (5.5; 6.0 and 6.4) dropped to approximately 60% in both, time zero (T0) and after 6 months (T6). This decrease might be related to the small amount of precipitation verified in these conditions, revealing a decrease in quantity of HBsAg particles available in solution, but not on its native conformation, supporting the results obtained by SRCD and fluorescence spectroscopies. Besides, the more acid pH could compromise the formation of the disulfide bonding, which is associated

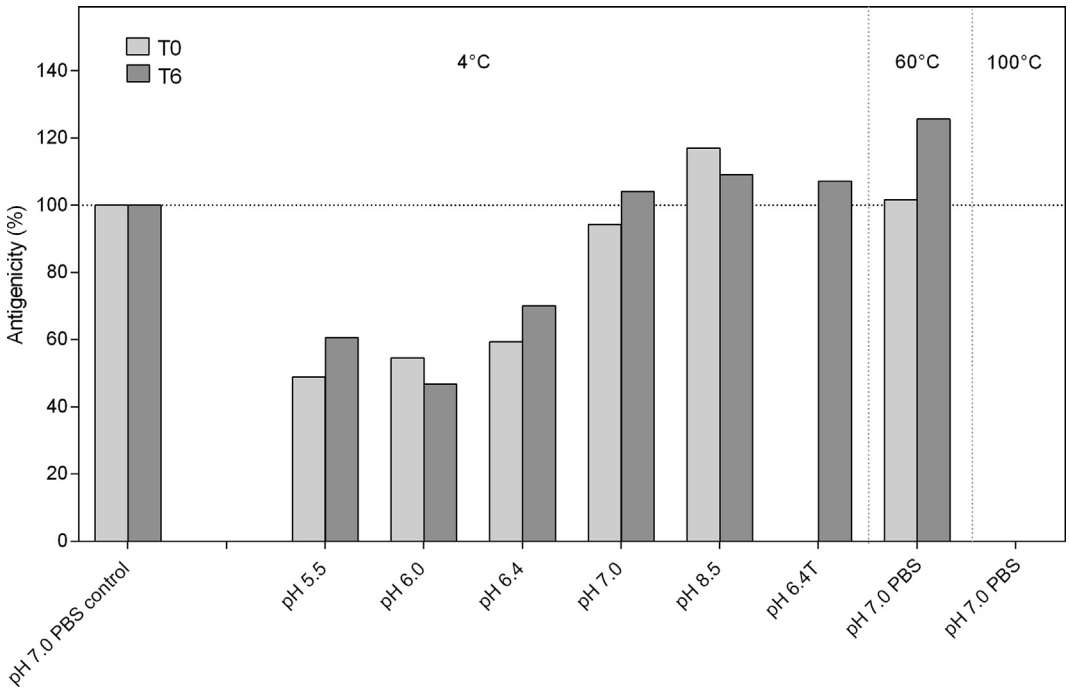

Fig. 6. Antigenicity of HBsAg in different pHs 5.5, 6.0, 6.4, 6.4 T, 7.0, 8.5 stored at 4 °C, pH 7.0 PBS stored at 60 °C and pH 7.0 PBS stored at 100 °C, in time 0 (T0) and after six months (T6), compared to antigenicity HBsAg control (pH 7.0 PBS).

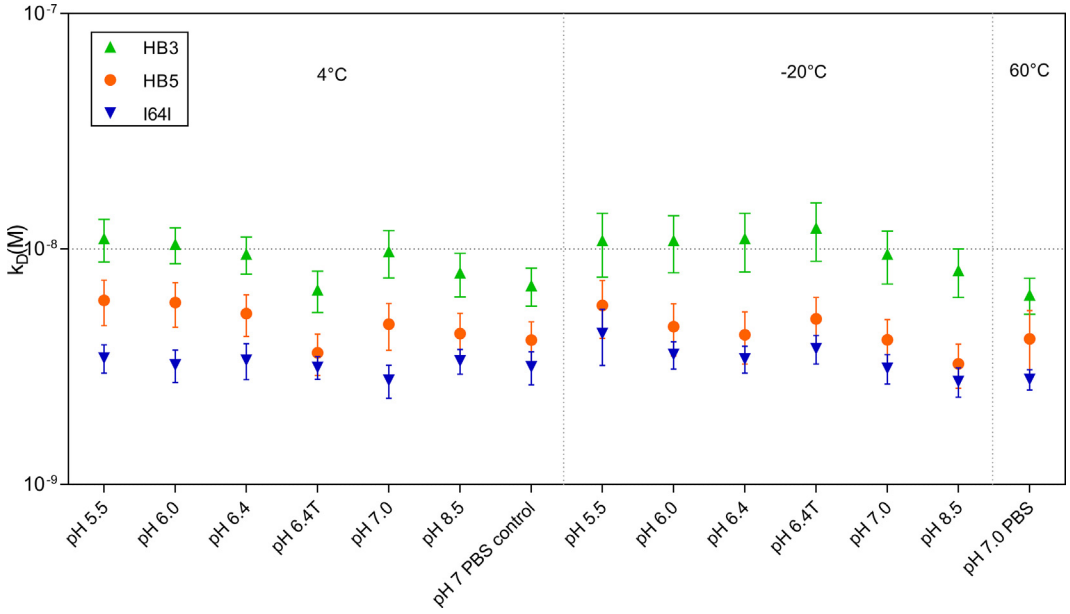

Fig. 7. Steady state affinity of HBsAg in different pH and strength ionic (sodium phosphate 10 mM pH 5.5, 6.0, 6.4, 6.4 T, 7.0 and 8.5, and PBS, pH 7.0) and, in different storage conditions (4 °C and −20 °C). Each point represents only one experiment and the error bar is the standard error provided by the Biacore T200 System software.

to the expression of important epitopes of HBsAg [34]. Instead, samples kept in the other pH and ionic strength conditions (solutions at pH 7.0, 8.5 and 6.4 T) maintained its potency, even after 6 months. All samples kept frozen at −20 °C precipitated when fast-thawed at room temperature and the results of HBsAg content were highly variable and could not be properly analyzed (data not shown). As showed by DLS method at this temperature a slightly larger amount of aggregates was described, which could be associated to loss of the vaccine potency [10,13]. Samples maintained at room temperature were not tested in the in vivo and in vitro assays due to problems occurred during storage.

3.6. Assay for in vitro antigen-antibody interaction by surface plasmon resonance (SPR) instrumentation

As the conformation of protein is crucial for the recognition of antibodies, it was also analyzed the antigen antibody interaction by SPR instrumentation of 3 different mAbs, directed against different epitopes of S protein (HB3, HB5 and I64I), with HBsAg particles in different conditions of preparation and storage. Storage conditions and pH did not affect HBsAg recognition by the different mAbs (Fig. 8), demonstrating the maintenance of the structural and morphology of the particle.

Please cite this article as: J. L. S. Lopes, D. C. A. Oliveira, C. L. A. Utescher et al., Antigenic and physicochemical characterization of Hepatitis B surface protein under extreme temperature and pH conditions, Vaccine, https://doi.org/10.1016/j.vaccine.2019.09.005

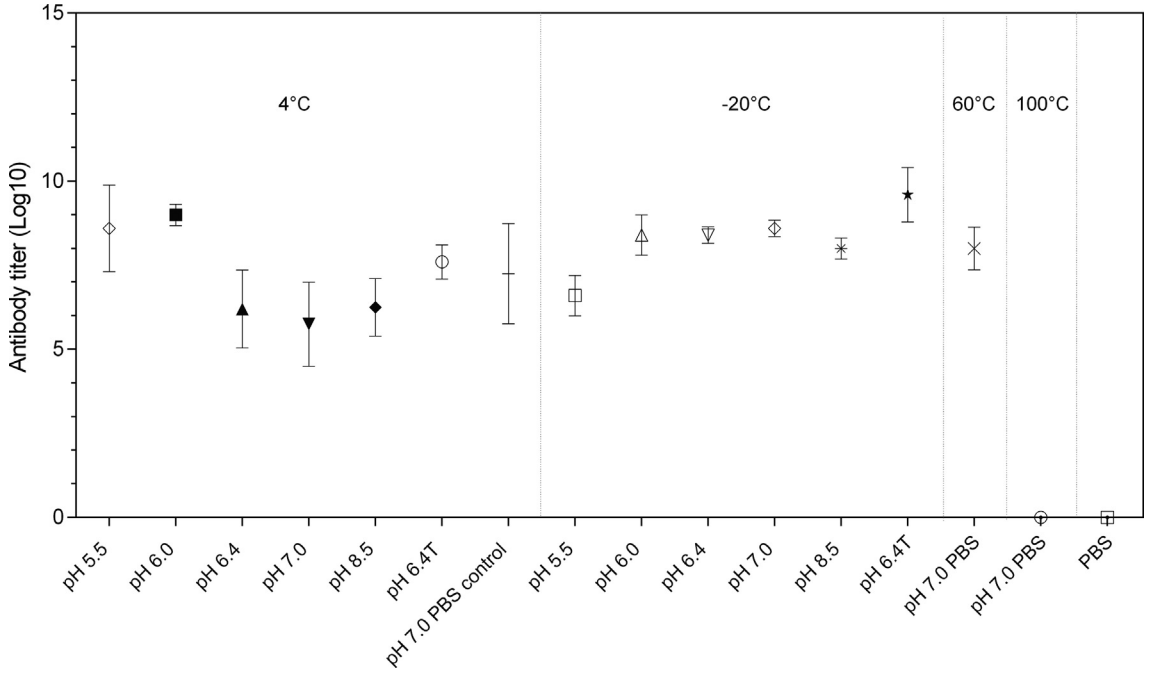

Fig. 8. Antibody titer of total IgG anti-HBsAg production in BALB/c mice intraperitoneally immunized with different formulations of HBsAg (different pH 5.5, 6.0, 6.4, 6.4 T, 7.0 and 8.5) and storage at 4 °C and −20 °C. Immune response of HBsAg particles is largely lost after heating at 100 °C ($p < 0.05$).

In vivo potency test: The ability of different formulations to induce total IgG anti-HBsAg response was performed in mice. All samples, in different pHs, ionic strength and different storage temperatures, induced similar immunological response when compared to the control reference, except the sample heated at 100 °C (Fig. 8), suggesting once again an important alteration of their structure and conformation at high temperature.

4. Conclusions

Bioinformatics analyses, fluorescence and SRCD spectroscopies indicate that HBsAg is indeed a well-ordered globular protein, which assumes a mixed α/β conformation in solution, preserving its Trp residues from solvent exposure. Scattering methods, SAXS and DLS, provided useful indications on overall protein size and shape and oligomeric state, indicating the stability of the protein for broad pH ranges. The native secondary and tertiary structure of HBsAg in solution remains quite stable for 6 months when kept at 4 °C or at room temperature (~20 °C) for 5 consecutive days, and the stability of the protein submitted to different pHs and ionic strength, ranging from 5.5 to 8.5, was also high. However, at frozen temperatures, both large aggregates (>200 nm) and protein precipitation were noticed, and that possibly causes the loss of HBsAg content, but it did not interfere in the affinity of the antigen with specific antibodies or in the in vivo assay. Some level of protein aggregation has also been observed at extreme pH levels, especially with the more acidic pHs, which might explain the loss of around 60% antigen content determined by ELISA. Aggregation did not interfere in the results of other biological tests. These results showed that the conformational structure of the protein, crucial for the developing of the immune response, has been preserved.

On the other hand, HBsAg can be unfolded by the effect of high temperature (especially after 45 °C), with remarkable conformational changes on its secondary structure after this point, although the immunogenic and antigenic properties at temperatures above this point are still preserved. Fully denaturation was observed only at the high temperature of 100 °C, verified by the total loss of antigenic and immunogenic properties. Finally, the incorporation of HBsAg into SBA-15 particles does not cause protein unfolding or any detectable conformational changes from its native state.

The combined results from all the characterization techniques proved that HBsAg is very stable under harsh temperatures (up to 45 °C) and pH conditions (5.5–8.5), an important finding for oral vaccine delivery at the Peyer's patches. The OMS SBA-15 scaffold could protect the antigen from the acidic stomach fluid, such that it can reach the intestine. In addition, the stability of HBsAg inside SBA-15 at room temperature (25 °C) might improve the distribution of the vaccine and consequently the efficiency of global vaccination programs.

Declaration of Competing Interest

The authors declare that they have no known competing financial interests or personal relationships that could have appeared to influence the work reported in this paper.

Acknowledgements

Authors are grateful for grants 406429/2016-2 from National Council for Scientific and Technological Development (CNPq/Brazil) to JLSL, and the beamline access to the AU-CD beamline on ASTRID2 at ISA Synchrotron (Aarhus, Denmark) to JLSL. The authors would like to acknowledge Dr. Ana Maria Moro for the kind support to SPR experiments. Thanks are due to the São Paulo Research Foundation (FAPESP) for the financial support (grants 2017/17844-8 and 2018/19546-7) and to The Danish Agency for Science, Technology and Innovation (International Network Programme – Ref. number: 5132-00054B). CLPO, JLSL, MCAF and OAS are CNPq fellows. This research is under the scope of the International Patents WO07/030901, IN 248654, ZA 2008/02277, KR 1089400, MX 297263, HK 1124791, JP 5091863, CN 101287491B, CA 2621373, US 8642258 B2, EP 1942934 B1 and BR PI 0503817-0.

Author contribution

V.F.B., J.L.S.L. and M.C.A.F. designed and supervised the project. C.L.P.O., M.K.R., and M.C.A.F. performed and analyzed the SAXS and DLS experiments. J.L.S.L. performed the SRCD and fluorescence spectroscopies experiments and analyzed the data. D.C.A.O., C.L.A. U, W.Q. and V.F.B. performed the biological tests (ELISA, in vivo potency, SPR, SDS-PAGE) and performed the data analysis. H.N.B. O.A.S. and E.C.N.T. participated in the discussions. M.C.A.F., V.F.B., J.L.S.L., M.K.R., H.N.B. and C.L.P.O. wrote the paper with input from all authors. The final version was approved by all.

Appendix A. Supplementary material

Supplementary data to this article can be found online at https://doi.org/10.1016/j.vaccine.2019.09.005.

References

[1] World Health Organization. Global Health Sector Strategy on viral hepatitis 2016-202Towards Ending viral hepatitis. Publication date: June 2016. https://www.who.int/hepatitis/strategy2016-2021/ghss-hep/en/. [accessed 7 February 2019].
[2] Hutin Y, Desai S, Bulterys M. Preventing hepatitis B virus infection: milestones and targets 443-443A. Bull World Health Organ 2018;96. https://doi.org/10.2471/BLT.18.215210.
[3] World Health Organization. Weekly Epidemiological Record No 27, update, 7 July 2017. https://apps.who.int/iris/bitstream/handle/10665/255841/WER9227.pdf;jsessionid=896E98D15EC26F5618F08660726F5E59?sequence=1; 2017 [accessed 7 February 2019].
[4] World Health Organization. Hepatitis B vaccines: WHO position paper, July 2017. Recommendations. Vaccine 2019;37(2):223–5. https://doi.org/10.1016/j.vaccine.2017.07.046.
[5] Zhao Q, Wang Y, Freed D, Fu TM, Gimenez JA, Sitrin RD, et al. Maturation of recombinant hepatitis B virus surface antigen particles. Hum. Vaccin. 2006;2(4):174–80.
[6] Chen Y, Zhang Y, Quan C, Luo J, Yang Y, Yu M, et al. Aggregation and antigenicity of virus like particle in salt solution-A case study with hepatitis B surface antigen. Vaccine 2015;33(35):4300–6. https://doi.org/10.1016/j.vaccine.
[7] Lang R, Winter G, Vogt L, Zurcher A, Dorigo B, Schimmele B. Rational design of a stable, freeze-dried virus-like particle-based vaccine formulation. Drug Dev Ind Pharm 2009;35:83–97. https://doi.org/10.1080/03639040802192806.
[8] World Heathy Organization. A systematic review of monovalent hepatitis B vaccine thermostability, 2016. <http://www.who.int/immunization/sage/meetings/2016/october/6_Thermostability_HBV_04102016.pdf?ua=1> [accessed 7 February 2019].
[9] Jezek J, Chen D, Watson L, Crawford J, Perkins S, Tyagi A, et al. A heat-stable hepatitis B vaccine formulation. Human Vaccines 2009;5(8):529–35. https://doi.org/10.4161/hv.5.8.8600.
[10] Braun LJ, Jezek J, Peterson S, Tyagi A, Perkins S, Sylvester D, et al. Characterization of a thermostable hepatitis B vaccine formulation. Vaccine 2009;27:4609–14. https://doi.org/10.1016/j.vaccine.2009.05.069.
[11] Van Damme P, Cramm M, Safary A, Vandepapelière P, Meheus A. Heat stability of a recombinant DNA hepatitis B vaccine. Vaccine 1992;10(6):366–7.
[12] World Heathy Organization. Recommendations to assure the quality, safety and efficacy of recombinant hepatitis B vaccines. WHO Technical report series No. 978. World Health Organization, Geneva, 2013. <http://www.who.int/biologicals/vaccines/TRS_978_Annex_4.pdf> [accessed 7 February 2019].
[13] Chen D, Tyagi A, Carpenter J, Perkins S, Sylvester D, Guy M, et al. Characterization of the freeze sensitivity of a hepatitis B vaccine. Human Vaccines 2009;5(1):26–32. https://doi.org/10.4161/hv.5.1.6494.
[14] Kumru OS, Joshi SB, Smith DE, Middaugh CR, Prusik T, Volkin DB. Vaccine instability in the cold chain: mechanisms, analysis and formulation strategies. Biologicals 2014;42(5):237–59. https://doi.org/10.1016/j.biologicals.2014.05.007.
[15] Lubeck MD, Davis AR, Chengalvala M, Natuk RJ, Morin JE, Molnar-Kimber K, et al. Immunogenicity and efficacy testing in chimpanzees of an oral hepatitis B vaccine based on live recombinant adenovirus. Proc Natl Acad Sci 1989;86(17):6763–7.
[16] Ishizaka S, Kuriyama S, Kikuci E, Nishimura K, Tsujii T. A novel oral adjuvant for hepatitis B virus (HBV) vaccines. J Hepatol 1990;11:326–9. https://doi.org/10.1016/0168-8278(90)90216-E.
[17] Hayden CA, Smith EM, Turner DD, Keener TK, Wong JC, Walker JH, et al. Supercritical fluid extraction provides an enhancement to the immune response for orally-delivered hepatitis B surface antigen. Vaccine 2014;32:1240–6. https://doi.org/10.1016/j.vaccine.2014.01.037.
[18] Hayden CA, Fischer ME, Andrews BL, Chilton HC, Turner DD, Walker JH, et al. Oral delivery of wafers made from HBsAg-expressing maize germ induces long-term immunological systemic and mucosal responses. Vaccine 2015;33:2881–6. https://doi.org/10.1016/j.vaccine.2015.04.080.
[19] Farhadian A, Dounighi NM, Avadi M. Enteric trimethyl chitosan nanoparticles containing hepatitis B surface antigen for oral delivery. Human Vaccines Immunothera 2015;11(12):2811–8. https://doi.org/10.1080/21645515.2015.1053663.
[20] Dinda AK, Bhat M, Srivastava S, Kottarath SK, Prashant CK. Novel nanocarrier for oral Hepatitis B vaccine. Vaccine 2016;34:3076–81. https://doi.org/10.1016/j.vaccine.2016.04.084.
[21] Scaramuzzi K, Tanaka GD, Mariano-Neto F, Garcia PRAF, Gabrili JJM, Oliveira DVA, et al. Nanostructured SBA-15 silica: an effective protective vehicle to oral hepatitis B vaccine immunization. Nanomed Nanotechnol Biol Med 2016;12:2241–50. https://doi.org/10.1016/j.nano.2016.06.003.
[22] Soares E, Jesus S, Borges O. Oral hepatitis B vaccine: chitosan or glucan based delivery systems for efficient HBsAg immunization following subcutaneous priming. Int J Pharma 2018;535:261–71. https://doi.org/10.1016/j.ijpharm.2017.11.009.
[23] Mercuri LP, Carvalho LV, Lima FA, Quayle C, Fantini MCA, Tanaka GS, et al. Ordered mesoporous milica SBA-15: a new effective adjuvant to induce antibody response. Small 2006;2(2):254–6. https://doi.org/10.1002/smll.200500274.
[24] Carvalho LV, Ruiz RC, Scaramuzzi K, Marengo EB, Matos JR, Tambourgi DV, et al. Immunological parameters related to the adjuvant effect of the ordered mesoporous silica SBA-15. Vaccine 2010;28:7829–36. https://doi.org/10.1016/j.vaccine.2010.09.087.
[25] Mariano-Neto F, Matos JR, Cides da Silva LC, Carvalho LV, Scaramuzzi K, Sant'Anna OA, et al. Physical properties of ordered mesoporous SBA-15 silica as immunological adjuvant. J Phys D: Appl Phys 2014;47(42):425402. https://doi.org/10.1088/0022-3727/47/42/425402.
[26] Zhao D, Feng J, Huo Q, Melosh N, Fredrickson GH, Chmelka BF, et al. Triblock Copolymer syntheses of mesoporous silica with periodic 50 to 300 Angstrom pores. Science 1998;279:548–52. https://doi.org/10.1126/science.279.5350.548.
[27] Garcia-Bennett AE. Synthesis, toxicology and potential of ordered mesoporous materials in nanomedicine. Nanomedicine 2011;6(5):867–77. https://doi.org/10.2217/nnm.11.82.
[28] Huang X, Young NP, Townley HE. Characterization and comparison of mesoporous silica particles for optimized drug delivery. Nanomater Nanotechnol 2014;4(2):1–15. https://doi.org/10.5772/58290.
[29] Zhang Q, Zhao Q, Zhang Y, Han N, Hu L, Zhang C, et al. Investigation of 3-D ordered materials with a high adsorption capacity for BSA and their potential application as an oral vaccine adjuvant. J Colloid Interface Sci 2014;434:113–21. https://doi.org/10.1016/j.jcis.2014.07.035.
[30] Rahikkala A, Pereira SAP, Figueiredo P, Passos MLC, Araújo ARTS, Saraiva MLMFS, et al. Mesoporous silica nanoparticles for targeted and stimuli-responsive delivery of chemotherapeutics: a review. Adv Biosyst 2018:1800020. https://doi.org/10.1002/adbi.201800020.
[31] Rasmussen MK, Kardjilov K, Oliveira CLP, Watts B, Villanova J, Botosso VF, et al. 3D visualization of hepatitis B vaccine in the oral delivery vehicle SBA-15. Sci Rep 2019;9:6106. , https://www.nature.com/articles/s41598-019-42645-5.
[32] Smith ML, Keegan ME, Mason HS, Shuler ML. Factors important in the extraction, stability and in vitro assembly of the hepatitis b surface antigen derived from recombinant plant systems. Biotechnol Prog 2002;18:538–50.
[33] Kikhney AG, Svergun DI. A practical guide to small angle X-ray scattering (SAXS) of flexible and intrinsically disordered proteins. FEBS Lett 2015;589:2570–7. https://doi.org/10.1016/j.febslet.2015.08.027.
[34] Wallace BA, Janes RW. Modern techniques for circular dichroism and synchrotron radiation circular dichroism spectroscopy. IOS Press; 2009. p. 231.
[35] Luna EJDA, Moraes JCD, Silveira L, Salinas HSN. Efficacy and safety of the Brazilian vaccine against Hepatitis B in newborns. Rev Saúde Pública 2009;43(6):1014–20.
[36] Lowry OH, Rosebrough NJ, Farr AL, Randal RJ. Protein measurement with the Folin phenol reagent. J Biol Chem 1951;193(1):265–75.
[37] Laemmli UK. Cleavage of structural proteins during the assembly of the head bacteriophage T4. Nature 1970;227:680–5.
[38] Oliveira CLP. Investigating macromolecular complexes in solution by small angle X-ray scattering, Current Trends in X-Ray Crystallography. In: Dr. Annamalai Chandrasekaran (Ed.), 2011, ISBN: 978-953-307-754-3. https://doi.org/10.5772/30730.
[39] Glatter O. Data evaluation in small angle scattering: calculation of the radial electron density distribution by means of indirect Fourier transformation. Acta Phys Austriaca 1977;47:83–102.
[40] Semenyuk AV, Svergun DI. GNOM – a program package for small-angle scattering data-processing. J Appl Crystallogr 1991;24:537–40. https://doi.org/10.1107/S002188989100081X.
[41] Svergun DI. Restoring low resolution structure of biological macromolecules from solution scattering using simulated annealing. Biophys J 1999;76(6):2879–86. https://doi.org/10.1016/S0006-3495(99)77443-6.
[42] Morrison ID, Grabowski EF, Herb CA. Improved techniques for particle-size determination by quasi-elastic light-scattering. Langmuir 1985;1(4):496–501. https://doi.org/10.1021/la00064a016.
[43] Miles AJ, Wallace BA. CDtoolX, a downloadable software package for processing and analyses of circular dichroism spectroscopic data. Protein Sci. 2018;27(9):1717–22. https://doi.org/10.1002/pro.3474.

Please cite this article as: J. L. S. Lopes, D. C. A. Oliveira, C. L. A. Utescher et al., Antigenic and physicochemical characterization of Hepatitis B surface protein under extreme temperature and pH conditions, Vaccine, https://doi.org/10.1016/j.vaccine.2019.09.005

[44] Whitmore L, Wallace BA. Protein secondary structure analyses from circular dichroism spectroscopy: methods and reference databases. Biopolymers 2008;89:392–400. https://doi.org/10.1002/bip.20853.

[45] Lees JG, Miles AJ, Wien F, Wallace BA. A reference database for circular dichroism spectroscopy covering fold and secondary structure space. Bioinformatics 2006;22(16):1955–62. https://doi.org/10.1093/bioinformatics/btl327.

[46] Sreerama N, Woody RW. Estimation of protein secondary structure from circular dichroism spectra: comparison of CONTIN, SELCON, and CDSSTR methods with an expanded reference set. Anal Biochem 2000;287:252–60. https://doi.org/10.1006/abio.2000.4880.

[47] Garnier J, Gibrat JF, Robson B. GOR method for predicting protein secondary structure from amino acid sequence. Methods Enzymol 1996;266:540–53. https://doi.org/10.1016/S0076-6879(96)66034-0.

[48] Almeida NL, Oliveira CLP, Torriani IL, Loh W. Calorimetric and structural investigation of the interaction of lysozyme and bovine serum albumin with poly(ethylene oxide) and its copolymers. Colloids Surf B - Biointerfaces 2004;38(1–2):67–76. https://doi.org/10.1016/j.colsurfb.2004.08.004.

[49] Glatter O. New method for evaluation of small-angle scattering data. J Appl Crystallogr 1977;10:415–21. https://doi.org/10.1107/S0021889877013879.

[50] Hirai M, Arai S, Iwase H, Takizawa T. Small-angle X-ray scattering and calorimetric studies of thermal conformational change of lysozyme depending on pH. J Phys Chem B 1998;102(7):1308–13. https://doi.org/10.1021/jp9713367.

[51] Erickson HP. Size and shape of protein molecules at the nanometer level determined by sedimentation, Gel Filtration, and Electron Microscopy. Biological Procedures Online 2009;11(1):32–51. https://doi.org/10.1007/s12575-009-9008-x.

[52] Jameson DM. Introduction to fluorescence. New York, NY: RC Press, Taylor and Francis Publishers; 2014.

[53] Greiner VJ, Manin C, Larquet E, Ikhelef N, Gréco F, Naville S, et al. Characterization of the structural modifications accompanying the loss of HBsAg particle immunogenicity. Vaccine 2014;32(9):1049–54. https://doi.org/10.1016/j.vaccine.2014.01.012.

[54] Carman WF. The clinical significance of surface antigen variants of hepatitis B virus. J Viral Hepat 1997;4(Suppl 1):11–20. Review. PubMed PMID: 9097273.

[55] Mulder AM, Carragher B, Towne V, Meng Y, Wang Y, Dieter L, et al. Toolbox for non-intrusive structural and functional analysis of recombinant VLP based vaccines: a case study with hepatitis B vaccine. PLoS ONE 2012;7(4):. https://doi.org/10.1371/journal.pone.0033235e33235.

Please cite this article as: J. L. S. Lopes, D. C. A. Oliveira, C. L. A. Utescher et al., Antigenic and physicochemical characterization of Hepatitis B surface protein under extreme temperature and pH conditions, Vaccine, https://doi.org/10.1016/j.vaccine.2019.09.005